

## SUPPORTING INFORMATION

### Photothermal Therapy with Silver Nanoplates in HeLa cells studied by in situ Fluorescence Microscopy

María Belén Rivas Ailello, Julio C. Azcárate, Eugenia Zelaya, Pedro David Gara,  
Gabriela N. Bosio, Thomas Gensch, and Daniel O. Mártire

#### Contents:

Figure S1: Size and shape of PVPAgNP.....	2
Figure S2: FTIR spectra of the nanoplates.....	3
Figure S3: MTT and NRU tests.....	3
Figure S4 and Table S1: Fluorescence spectra, fluorescence decays and fluorescence lifetimes of RhB with and without PVPAgNP.....	4
Figure S5: Fluorescence imaging of HeLa cells transfected with Dendra2-mito and incubated with RhB .....	5
Figure S6 and Table S1: Chart explaining the different ways to quantify RhB intensity of HeLa cells.....	7
Figure S7 and Table S2: Effect of 640 nm irradiation on the fluorescence intensity of HeLa cells incubated with 2.5 $\mu$ M RhB (30 min) in the absence of PVPAgNP.....	8
Figure S8: Examples of the three fluorescence decay types found in RhB-stained HeLa cells incubated with PVPAgNP.....	9
Figure S9: FLIM images of HeLa cells incubated with RhB, PVPAgNP and $\text{NaN}_3$ .....	10

### Figure 1: Size and Shape of PVPAgNP

The criterion adopted to characterize the size and shape of non-regular shape particles is mean diameter. The mean diameter is determined by minimum diameter of a circle inside the contour and the maximum diameter outside the contour of the polygonal shape. This determination was performed by the software iTEM (ResAlta).

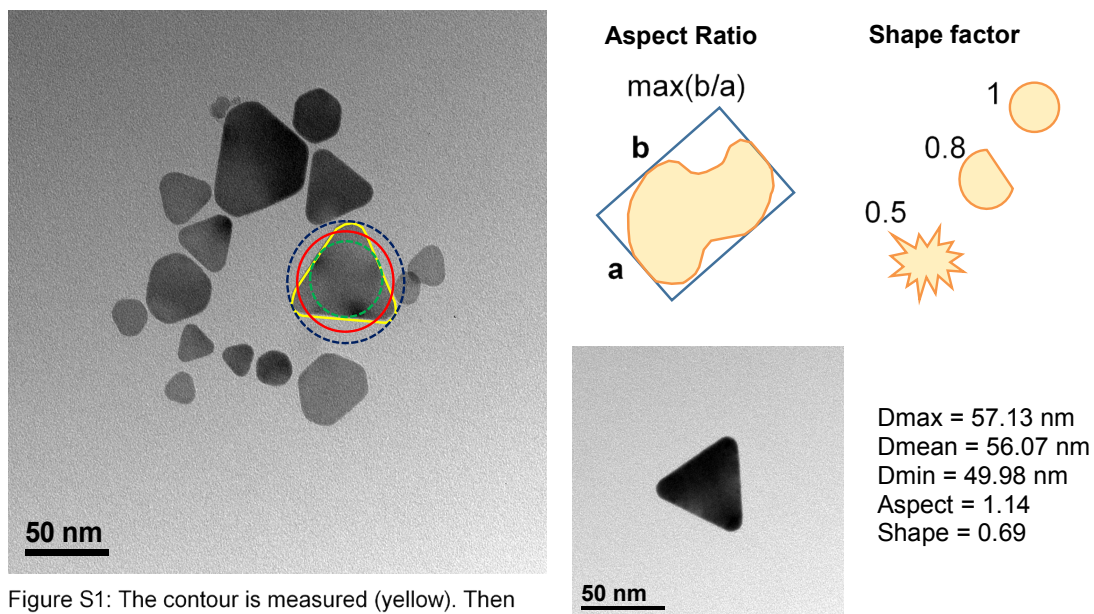
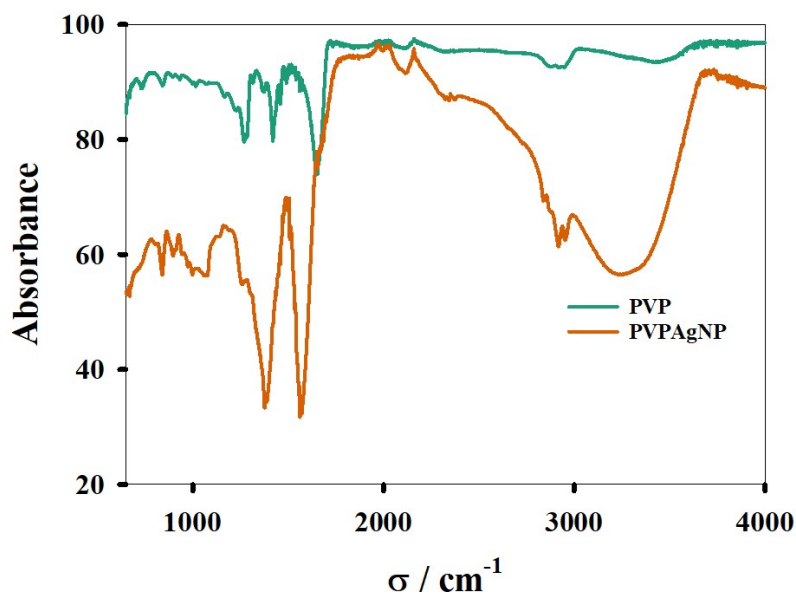
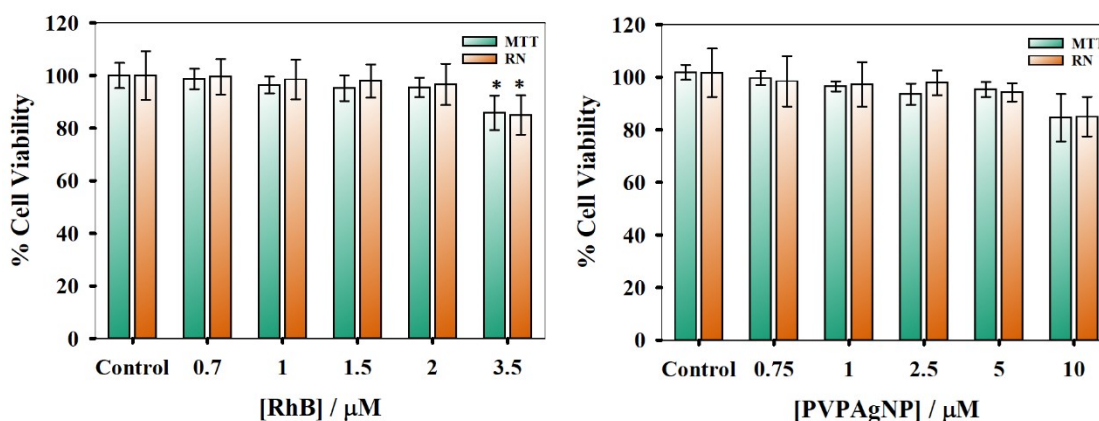


Figure S1: The contour is measured (yellow). Then the minimum insides circle (green) and the maximum outside circle (blue) is calculated to obtain the mean diameter (red).



**Figure S2:** ATR-FTIR spectra of PVP (green) and PVPAgNP (orange)



**Figure S3:** Histograms showing the results of the MTT (green) and NRU (orange) assays on HeLa cells incubated with different concentrations of RhB (a) and PVPAgNP (b), present in the incubation medium. Values of formazan and neutral red absorbance were normalized against average values obtained from cells to which neither RhB or particles had been added (control). Error bars refer to one standard deviation; in each case, the number of samples examined was at least 4 and as large as 6. No statistically significant difference was obtained between the different samples number and the number obtained from the control), except for 3.5 μM RhB, as indicated by the asterisk. (one-way ANOVA with Tukey's posthoc test;  $p < 0.05$ ).

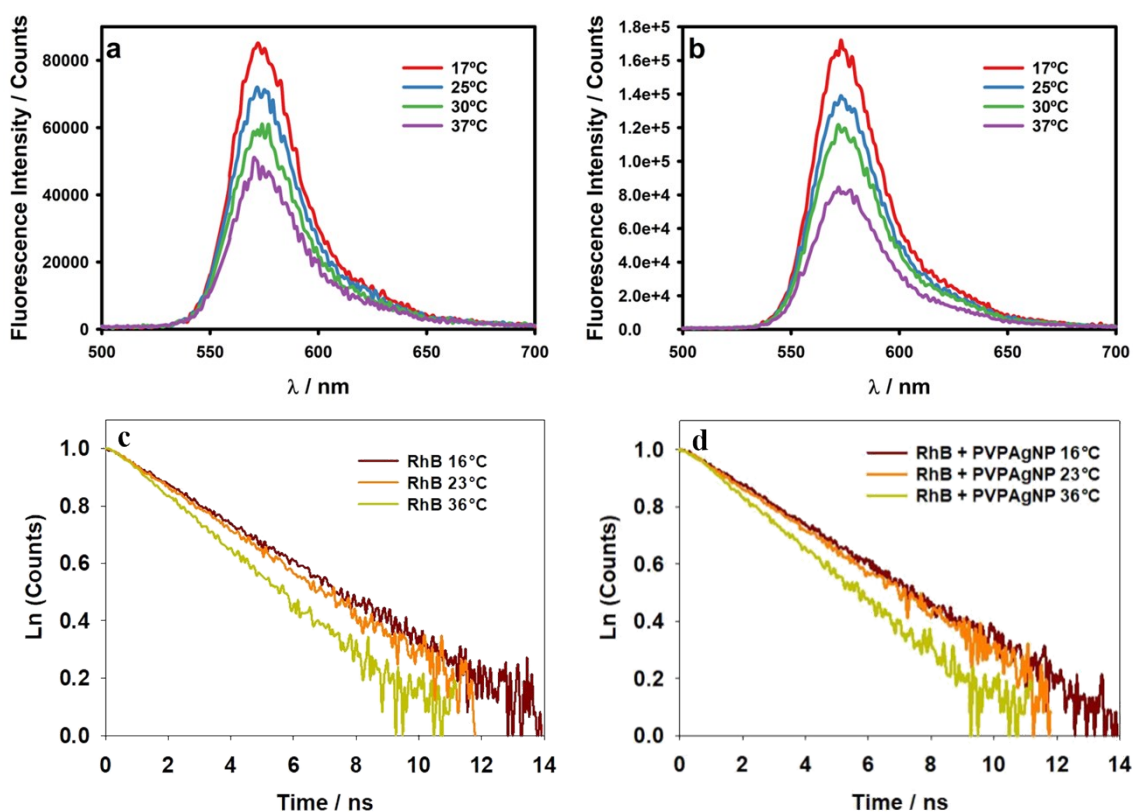


**Figure S4:** Fluorescence spectra and fluorescence decays of RhB with (a, c) and without PVPAgNP (b, d) at different temperatures.

**Table S1.** Fluorescence lifetime of RhB in the absence and presence of PVPAgNP at different temperatures. The standard deviation amounts to  $\pm 0.05$  ns (three repetitions for each condition).

	16°C	23°C	36°C
RhB	1.84 ns	1.61 ns	1.27 ns
RhB + PVPAgNP	1.82 ns	1.59 ns	1.30 ns

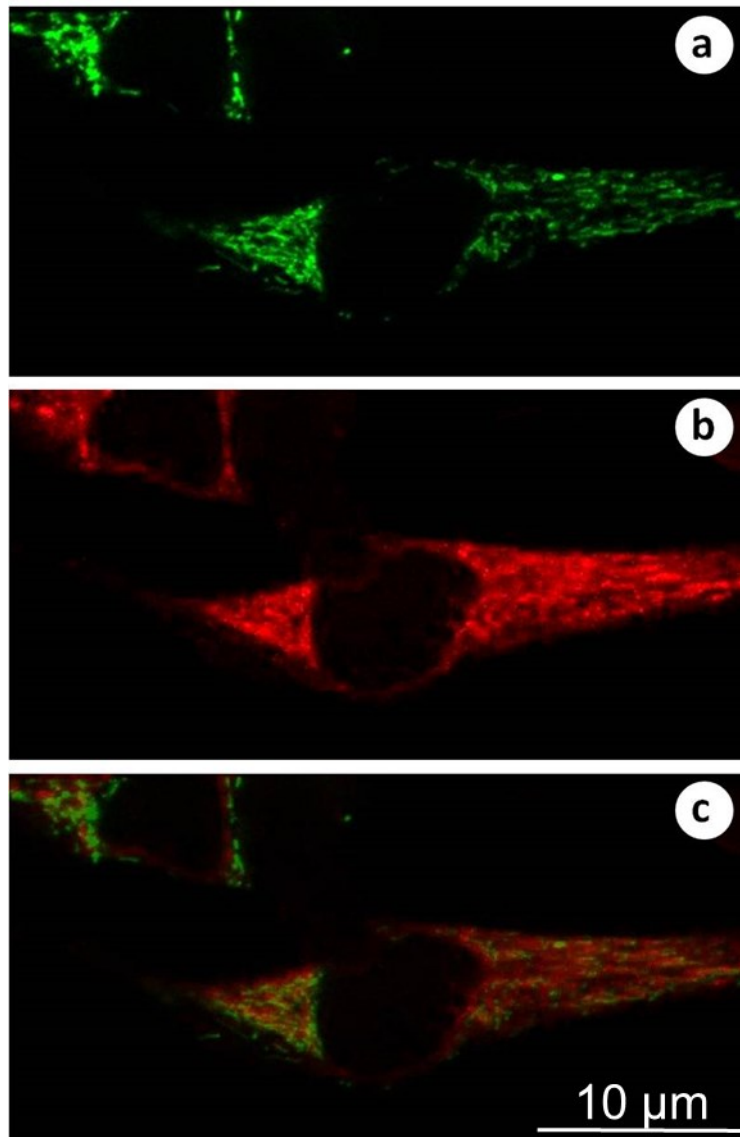


**Figure S5:** Fluorescence imaging of HeLa cells transfected with Dendra2-mito and also incubated with RhB: (a) The excitation wavelength for Dendra2-mito was 488 nm (137  $\mu$ W) and the emission wavelength was between 502.5 – 537.5 nm. (b) The excitation wavelength for RhB was 561 nm (3  $\mu$ W), and the emission was detected between 590 – 650 nm. (c) Superposition of the two images is shown in (a) and (b).

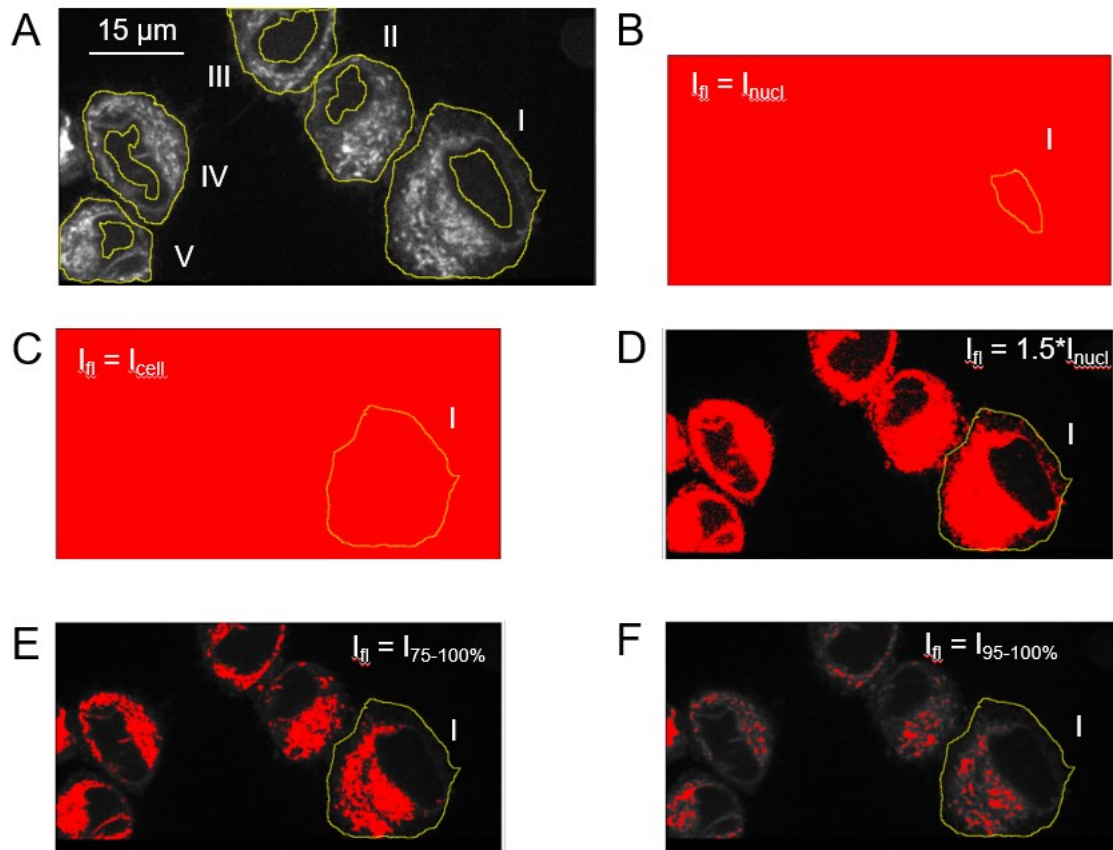


**Figure S6.** Chart explaining the different ways to quantify RhB fluorescence intensity of HeLa cells incubated with 2.5  $\mu\text{M}$  RhB (30 min). (A) shows the fluorescence images of five cells (same as in figure 5A (right picture)) with two regions of interest for every cell – one from within the nucleus and the other encircling the whole cell. The highly non-homogeneous spatial distribution of RhB with low (but not zero) signal from the nucleus, large signal from mitochondria (see figure S5) and medium signal from the rest of the cytoplasm required a detailed and comprehensive search to find the best measure that represents the average RhB fluorescence intensity of a cell at multiple time points. Other challenging points are changes of the cell morphology (relative area of nucleus compared to whole cell area) and the large mobility as well as fusion and fission of the mitochondria, the last being the areas (pixels) with largest impact on the fluorescence signal of the cell, which add an unwanted temperature-independent contribution. Five different ways to determine in a reliable measure for the cell's fluorescence intensity in such a complicated situation are graphically explained in (B-F): (B) average value of fluorescence intensity of the cell's nucleus ( $I_{\text{nuc1}}$ ); (C) average value of fluorescence intensity of the whole cell ( $I_{\text{cell}}$ ); (D) average value of fluorescence intensity of all pixels with a fluorescence larger than  $1.5 \cdot I_{\text{nuc1}}$  ( $I_{1.5 \cdot I_{\text{nuc1}}}$ ); (E) average value of fluorescence intensity of the pixels with fluorescence in the upper quartile ( $I_{75-100\%}$ ); (F) average value of fluorescence intensity of the most bright (5%) pixels ( $I_{95-100\%}$ ). These values and their standard deviations are listed in Table S1 for the five cells. The simplest way,

average of fluorescence intensity of the whole cell ( $I_{\text{cell}}$ ), has the largest relative standard deviation and suffers most from the heterogeneous signal distribution and the dynamics of cell morphology and mitochondria.  $I_{75-100\%}$  and  $I_{95-100\%}$  seem to represent purely fluorescence from the mitochondria – either all or only the most intense parts, respectively, with smaller relative standard deviations. The choice of 75 % and 95 %, however, was arbitrary and did not fit well for other cells analyzed, i.e., would have to be optimized for every experiment adding a human selection to the analysis. Also, these two measures are most vulnerable to changes in the mitochondria dynamics and morphology.  $I_{\text{nuc}}$  delivered also a stable readout of fluorescence with low relative standard deviation, but the fluorescence signal as such is rather low (only 2-3 times larger compared to the signal from “dark”, cell-free areas in the image). Also, many dyes have specific interactions with DNA- or other structures in the nucleus, where RhB has not been characterized in this respect. We therefore decided to define yet another value averaging the fluorescence from all pixels with a fluorescence intensity 50% larger compared to the average fluorescence intensity of the nucleus ( $I_{1.5*I_{\text{nuc}}}$ ). With this definition  $I_{1.5*I_{\text{nuc}}}$  represented very well the average fluorescence intensity from a large part of the cytoplasm including all mitochondria in all investigated cells. It gave very robust readings when the same cell was analyzed in subsequently recorded images.  $I_{1.5*I_{\text{nuc}}}$  was chosen as the fluorescence parameter of choice for representation of the cell’s fluorescence intensity and gave good results for determining (relative) temperature changes. We have to add here, that  $I_{\text{nuc}}$  gave quite similar results in experiments where we analyzed both, so  $I_{\text{nuc}}$  and  $I_{1.5*I_{\text{nuc}}}$  are similarly well suited when using RhB fluorescence intensity for temperature measurements.

**Table S2** Different quantitative measures for the average fluorescence intensity  $I_{\text{fl}}$  of the five cells from Figure S6A.

Cell	$I_{\text{nuc}}$ (SD)	$I_{\text{cell}}$ (SD)	$I_{1.5*I_{\text{nuc}}}$ (SD)	$I_{75-100\%}$ (SD)	$I_{95-100\%}$ (SD)
I	1923 (428)	3991 (2481)	5796 (2222)	7622 (1760)	10394 (1091)
II	2326 (475)	4548 (2337)	5812 (2180)	7797 (2064)	11021 (2042)
III	2295 (434)	3770 (1911)	5481 (1730)	6440 (1591)	9060 (1126)
IV	1956 (444)	4386 (2061)	5261 (1889)	7254 (1460)	9653 (1120)
V	2456 (451)	5056 (2632)	6588 (2337)	8810 (1898)	11804 (1383)



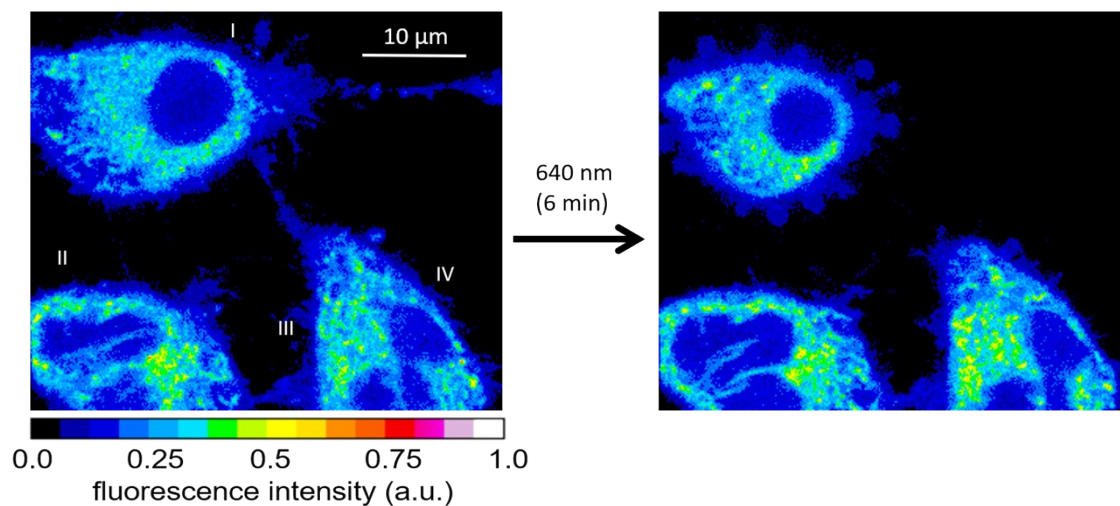


**Figure S7:** Effect of 640 nm irradiation on the fluorescence intensity of HeLa cells incubated with 2.5 μM RhB (30 min) in the absence of PVPAgNPs. Fluorescence intensity images ( $\lambda_{\text{exc}}=561$  nm) obtained before (left), and after 6 min (right) of 640 nm irradiation.

**Table S3** Average fluorescence intensity  $I_{\text{fl}} = I_{1.5} \cdot I_{\text{nucl}}$  of the four cells shown in Figure S7.

Cell	$I_{\text{fl, before 640 nm}}$	$I_{\text{fl, 640 nm (6 min)}}$
I	10157	10502 (3.4 %)
II	11661	11512 (- 1.3%)
III	12138	12321 (1.5 %)
IV	10952	11209 (2.3 %)



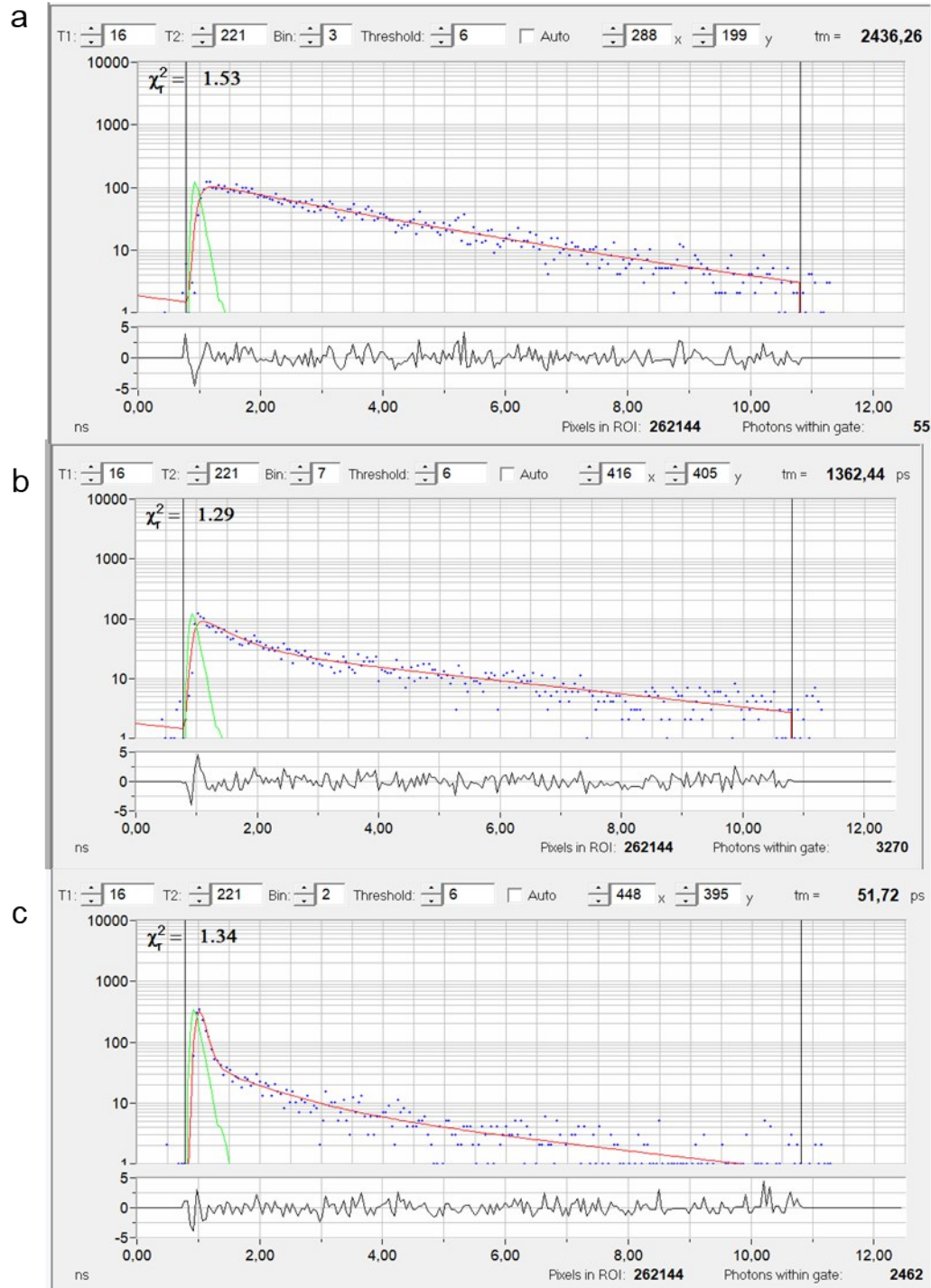


**Figure S8:** Examples of the three fluorescence decay types found in RhB-stained HeLa cells incubated with  $10 \mu\text{M}$  PVPAgNP with two-photon excitation ( $\lambda_{\text{exc}} = 880 \text{ nm}$ ): a) from mitochondria, where RhB is mainly localized (Fig. 7 d, f; 8 d, f). b) typical autofluorescence signal from HeLa cells after photobleaching of RhB (Fig. 7 f; 8 f). c) very short, multiexponential fluorescence decay from the intense, roundish fluorescent regions generated by illumination with fs-pulsed 780 nm light (only) in HeLa cells that were incubated with PVPAgNP (Fig. 7 f). Similar, very short, multiexponential decays can be observed, when excitation occurs at 780 nm (Fig. 7 e).

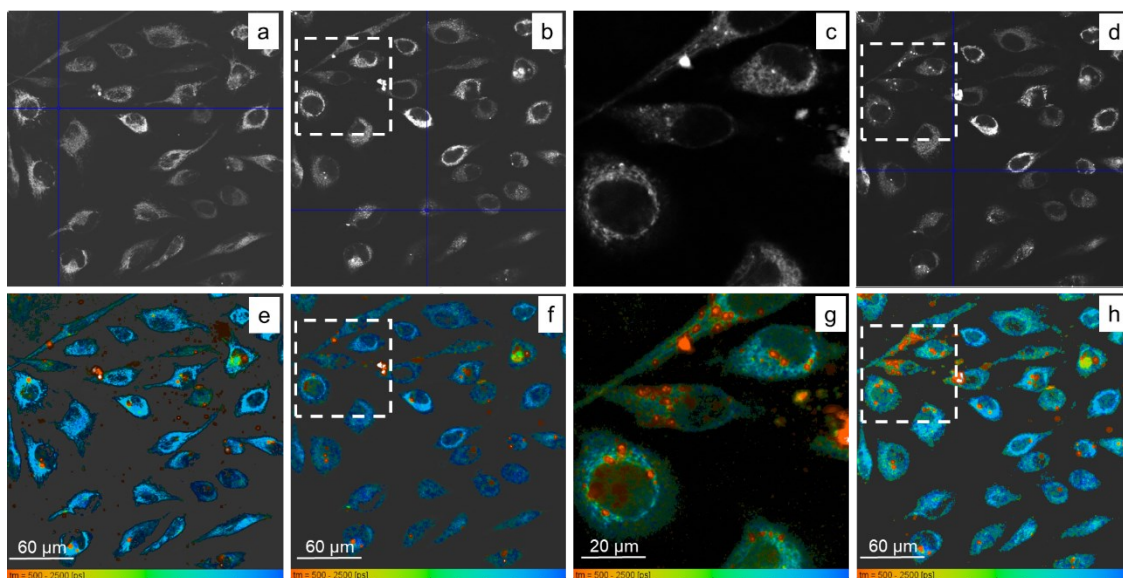


**Figure S9:** Fluorescence intensity and lifetime images of HeLa cells incubated with 10  $\mu\text{M}$  PVPAgNP (24h) and 0.5  $\mu\text{M}$  RhB (30 min) before (a, e) and after (b, f), (c, g) and (d, h) the addition 0.5mM of  $\text{NaN}_3$  (10 min). Images (a, e), (b, f), and (d, h) were obtained with 880 nm excitation and zoom 2. The area marked in white in (b, f) and (d, h) corresponds to the area (zoom 6) scanned by 780 nm light shown in (c, g) (illumination time 80s). Images (d, h) were obtained with 880 nm excitation and zoom 2 after recording image (c, g).